Evans, D. F., T. Tominaga, and C. Chan, "Diffusion of Symmetrical and Spherical Solutes in Protic, Aprotic and Hydrocarbon Solvents," *J. Solution Chem.*, **8**, p. 461 (1979).
Hayduk, W., and S. Cheng, "Review of Relation between Diffusivity and Solvent Viscosity in Dilute Liquid Solutions," *Chem. Eng. Sci.*, **26**, p. 635 (1971).
Hildebrand, J. H., and M. Ross, "Diffusion of Hydrogen, Deuterium, Nitrogen, Argon, Methane and Carbon Tetrachloride in Carbon Tetrachloride," *J. Chem. Phys.*, **40**, p. 2397 (1964).
Hildebrand, J. H., "Motions of Molecules in Liquids: Viscosity and Diffusivity," *Science*, **174**, p. 490 (1971).
Jonas, J., and H. J. Parkhurst, Jr., "Dense Liquids. I. The Effects of Density and Temperature on Self-Diffusion of Tetramethylsilane and Benzene-d_6," *J. Chem. Phys.*, **63**, p. 1698 (1975).
Jonas, J., and J. A. Akai, "Transport Processes in Compressed Liquid Methanol," *J. Chem. Phys.*, **66**, p. 4946 (1977).
Lusis, M. A., and G. A. Ratcliff, "Diffusion of Inert and Hydrogen-Bonding Solutes in Aliphatic Alcohols," *AIChE J.*, **17**, p. 1492 (1971).
Sakai, Y., Y. Sadaoka, and T. Yamamoto, "Temperature Dependence of Association of Methanol, Ethanol, and 1-Propanol," *Bull. Chem. Soc. Japan*, **46**, p. 3575 (1973).
Taylor, G. I., "Dispersion of Soluble Matter in Solvent Flowing Slowly through a Tube," *Proc. Roy. Soc.* (London), **A219**, p. 186 (1953).
Van der Laan, E. Th., "Notes on the Diffusion-Type Model for the Longitudinal Mixing in Flow," *Chem. Eng. Sci.*, **7**, p. 187 (1958).
Wilhelm, E., "On the Temperature Dependence of the Effective Hard Sphere Diameter," *J. Chem. Phys.*, **58**, p. 3558 (1973).
Wilke, C. R., and P. R. Chang, "Correlations of Diffusion Coefficients in Dilute Solutions," *AIChE J.*, **1**, p. 264 (1955).

Manuscript received July 24, 1981; revision received March 12, and accepted March 23, 1982.

Variable Volume Enzyme Reactor with Ultrafiltration Swing: A Theoretical Study on CSTR Case

IN HO KIM and HO NAM CHANG

**Department of Chemical Engineering
Korea Advanced Institute of Science and Technology
Seoul, Korea**

A new membrane enzyme reactor system is proposed, and its performance is analytically and numerically examined by operational modes. This membrane-separated, two-compartmental reactor is operated in a cyclic manner such that ultrafiltration swing is induced either by a pulsatile flow or by an alternating pressure difference. Substrate and product solutions are permeable to the membrane while enzyme is impermeable. In one reservoir, enzyme solution is stored into which substrate is supplied by diffusion-coupled ultrafiltration and product is removed by the same mechanism into the substrate compartment, which is similar to CSTR in view of fluid mixing and continuous inlet-outlet flows, but differs from CSTR in a sense that reaction takes place only in the enzyme compartment.

The governing model equations are derived and their analytical solutions are obtained for fast reaction and high ultrafiltration with first-order kinetics. In addition, nonlinear Michaelis-Menten kinetics problem is solved numerically. As a result, we have found that the system can increase the conversion substantially compared with previous diffusion-moderated enzyme reactors where diffusion very often can limit the extent of conversion.

SCOPE

In the last decade, several membrane devices have been considered for an immobilized enzyme reactor where soluble form of enzymes can be retained. This effort stems from the fact that insolubilization of enzymes requires chemical modification of supports and purification of enzymes to such extent that sometimes the whole process may become uneconomical. Despite these troublesome procedures, the recovery of the original enzyme activity is very often minimal. For this reason physical immobilization technique will be favorably sought if we have a method to keep a native enzyme stable in a soluble form (Schmid, 1979).

Hollow-fiber devices are used to retain an enzyme solution in the shell or lumen and a substrate solution flows in the opposite side (Waterland et al., 1974; Rony, 1971). On the other hand, ultrafiltration cells are used as CSTR where substrates and enzymes are mixed to react and only the product is removed through the membrane by ultrafiltration (Butterworth et al., 1970), or substrate passes through the immobilized enzyme membrane (Alfani et al., 1979). In spite of the promising role of these membrane devices as immobilized enzyme reactor a certain aspects of operational limitations are unavoidable. In the hollow-fiber reactor, the flow rate has to be low to achieve a considerable conversion since diffusion often limits the conversion. Besides, washing-out of enzymes from the sponge region of the fiber frequently happens to cause unequal distribution of enzymes along the fiber. The water flux in the ultrafiltration cell is also limited owing to the concentration polarization near the membrane surface.

In this study we propose a new membrane enzyme reactor having operational flexibility by combining the features of hollow-fiber device and ultrafiltration cell. This reactor is operated with ultrafiltration of an alternating direction which is induced either by an alternating pressure difference or by a pulsatile flow at the inlet or outlet of the substrate compartment. For the systematic investigation a theoretical model was developed to evaluate the performance of the new variable volume membrane enzyme reactor system by its various operational modes.

Correspondence concerning this paper should be addressed to H. N. Chang.

CONCLUSION AND SIGNIFICANCE

The analysis of a theoretical model has proved that this reactor can substantially enhance the performance of the conventional diffusion moderated reactor. Analytical solutions are obtained for the high ultrafiltration case with first-order kinetics. By varying the parameter "β," the measure of convectional transport to diffusional transport, we can see that the conversion can reach as high as that of CSTR at high β. This effect becomes more noticeable especially in the diffusion controlled region of high Damköhler number ($\lambda^2 \gg 1$). The first-order high ultrafiltration approximation agrees with the numerical solution of first-order kinetics for $\beta > 5$.

Analytical solutions for the fast reaction are also derived to compare the features of various modes of ultrafiltration swing. The solutions show that the pulsatile flow results in higher conversion than that of the pressure swing at a large fractional volume change. At a low fractional volume change the conversions of the pressure swing and the flow swing approach each other. However, the flow swing has an operational restriction that the mean flow rate has to be larger than the ultrafiltration rate.

The theoretical results of the present study clearly show that the ultrafiltration swing provides the membrane enzyme reactor with flexible operational methods for efficient enzymic reaction.

To eliminate diffusional limitation, Furusaki et al. (1977) proposed a new enzyme reactor resembling a batch diffusion cell in which cyclic pressure difference was applied between the two compartments containing enzyme and substrate, respectively. This led to forward and backward convective transport of substrate and product through the membrane. Experiments were performed with catalyst and hydrogen peroxide, and the experimental data were fitted to the simple theory of their own. However, the assumptions used in the mathematical development are so qualitative that the theory can not be successfully used to study the phenomena ocurring in the reactor in detail. Recently, Ku et al. (1981) reported their experimental data of a pulsed flat-bed hollow-fiber culture system consisting of rectangular-shaped hollow-fiber device, pressurizing equipment and vacuum generating device to supply air in lumen to cells in shell side.

These two studies lack elaborate analysis to predict the experimental data and examine the behavior of the reactor. As an initial effort to understand the convection-moderated enzyme reactor quantitatively, Chang and Kim (1981) performed a brief numerical analysis on the pressure swing operation by simulating a model equation, which concluded that higher conversion can be attained with the pressure swing operation. In the present investigation, in addition to the pressure swing, we have introduced another ultrafiltration swing method which can be induced by a pulsatile flow at the inlet or the outlet of the reactor. To develop a general theory on the variable volume enzyme reactor, a lumped model will be introduced. This analysis may serve as design and operation models for a new category of hollow-fiber enzyme reactors.

PROPOSED METHOD FOR INDUCING ULTRAFILTRATION

A schematic model for the variable volume enzyme reactor is shown in Figure 1. Using solenoid valves with timer, pressure can be applied alternatively to both compartments separated by a membrane to which the enzyme in region 2 is impermeable. On the other hand, the substrate in region 1 can enter into the region 2 by diffusion and convection and react with the enzyme. Furusaki et al. (1977) operated the reactor in a batch mode; however, it may be operated in a continuous mode by feeding substrate solution into region 1 from which the same amount is withdrawn. It is also assumed that each compartment is well mixed and there is no concentration gradient.

In addition, it is pertinent to propose a new method for ultrafiltration swing. Without using the pressurizing equipment, we can produce ultrafiltration by holding either inflow or outflow rate constant at mean flow rate and maintaining the other stream above or below the mean flow periodically. In Figure 2, schematic diagrams representing the methods for inducing ultrafiltration are illustrated. Mode I is the first mentioned pressure swing, and modes II and III are the flow swing methods. During forward cycle, forward ultrafiltration occurs due to the difference between the inlet and the outlet flow rate, and backward ultrafiltration takes place in the same manner.

The realization of flow swing for the mode III can be achieved by using three independent pumps. Two inlet pumps, of which flow rates are fixed high and low respectively, are connected to a timer from which actuating signal comes periodically and the remaining outlet pump is set to the average flow rates of the two inlet pumps. The flow swing has a practical advantage over the pressure swing in that volume of substrate compartment can be kept at a constant level. When we utilize a hollow-fiber device as the variable volume enzyme reactor, the lumen of fibers may be employed as substrate compartment. Hence the feature of large surface area to volume can be suitable for the variable enzyme reactor instead of the diffusion cell.

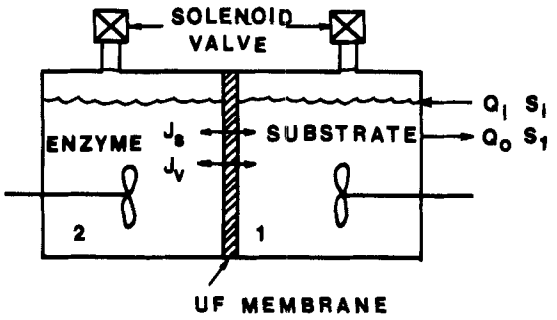

Figure 1. Schematic diagram of variable volume enzyme reactor.

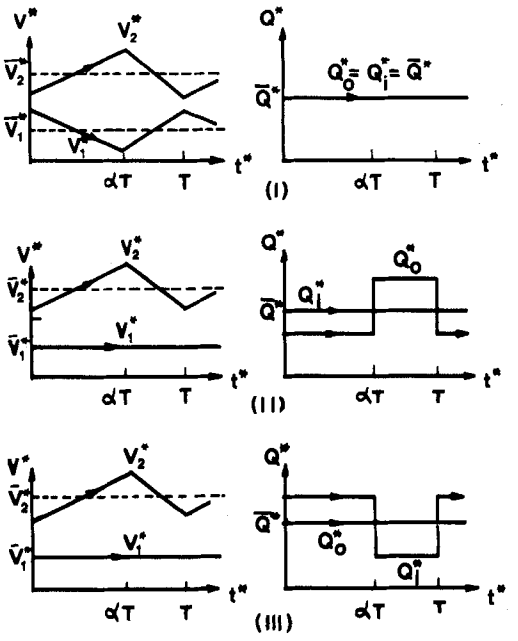

Figure 2. Operation modes of variable volume enzyme reactor.

TABLE 1. DIMENSIONLESS VARIABLES IN OPERATION SCHEME OF VARIABLE VOLUME ENZYME REACTOR

Mode	Time	Q_1	Q_2	V_1	V_2
I	Forward	F	F	$1 + \frac{1}{4}\theta\beta - \theta\beta_f t$	$r - \frac{1}{4}\theta\beta + \theta\beta_f t$
	Backward	F	F	$1 - \frac{1}{4}\theta\beta + \theta\beta_b(t-\alpha)$	$r + \frac{1}{4}\theta\beta - \theta\beta_b(t-\alpha)$
II	Forward	F	$F - \theta\beta_f$	1	$r - \frac{1}{4}\theta\beta + \theta\beta_f t$
	Backward	F	$F + \theta\beta_b$	1	$r + \frac{1}{4}\theta\beta - \theta\beta_b(t-\alpha)$
III	Forward	$F + \theta\beta_f$	F	1	$r - \frac{1}{4}\theta\beta + \theta\beta_f t$
	Backward	$F - \theta\beta_b$	F	1	$r + \frac{1}{4}\theta\beta - \theta\beta_b(t-\alpha)$

$t = t^*/T \quad \theta\beta = AJ_oT/\bar{V}_1^* \quad F = \bar{Q}^*T/\bar{V}_1^*$

MATHEMATICAL DEVELOPMENT

The idealized model of membrane enzyme reactor consists of two regions where complete mixing is assumed: Region 1 is the substrate compartment, and region 2 is the enzyme reservoir where enzymic reaction takes place. Assuming the difference in the osmotic pressure between the two region is small, the solvent and solute fluxes J_v, J_s are written as

$$J_v = k\Delta P = u \tag{1}$$

$$J_s = -D\frac{dS^*}{dz} + uS^* \tag{2}$$

where ΔP, u and D are respectively the applied pressure difference between the compartments, permeation velocity through the membrane, and the substrate diffusivity. Provided that the transport through membrane is slow enough compared with the concentration change in the both region, Eq. 2 may be integrated to yield

$$J_s = \frac{u(S_1^* \exp(u/u_d) - S_2^*)}{\exp(u/u_d) - 1} \tag{3}$$

where $u_d = D/l$, l is the effective diffusion length in the membrane (Bean, 1972).

The governing differential equations for substrate concentration in each region are

$$\frac{d(V_1^*S_1^*)}{dt^*} = -AJ_s + Q_i^*S_i^* - Q_o^*S_1^* \tag{4}$$

$$\frac{d(V_2^*S_2^*)}{dt^*} = AJ_s - V_2^*R \tag{5}$$

The rate of the enzymatic reaction is usually described by the Michaelis-Menten expression:

$$R = \frac{V_mS_2^*}{K_m^* + S_2^*} \tag{6}$$

Introducing the following dimensionless variables,

$$K_m = K_m^*/S_i^*, \quad S_1 = S_1^*/S_i^*, \quad S_2 = S_2^*/S_i^*,$$

$$Q = Q^*T/\bar{V}_1^*, \quad F = \frac{\bar{Q}^*T}{\bar{V}_1^*}t = t^*/T, \quad \beta = u/u_d,$$

$$\theta = F_m^*T/\bar{V}_1^*, \quad \lambda^2 = V_m\bar{V}_2^*/S_i^*F_m^*$$

where $F_m^* = AD/l$, we can transform Eqs. 4 and 5 into the following dimensionless forms:

$$\frac{d(V_1S_1)}{dt} = -\frac{\theta\hat{\beta}}{e^{\hat{\beta}} - 1}(e^{\hat{\beta}}S_1 - S_2) + Q_i - Q_oS_1 \tag{7}$$

$$\frac{d(V_2S_2)}{dt} = \frac{\theta\hat{\beta}}{e^{\hat{\beta}} - 1}(e^{\hat{\beta}}S_1 - S_2) - \frac{\theta\lambda^2S_2}{K_m + S_2} \tag{8}$$

The ratio of convective flux to diffusive flux is expressed as $\hat{\beta} = \beta_f$ during forward cycle and $\hat{\beta} = -\beta_b$ during backward cycle. The relations among β, β_f, and β_b are described by $\beta_f = (1-\alpha)\beta_b$ and $\beta = 2\alpha\beta_f$ to keep the mean volume of region 2 at $\bar{V}_2^*$. In Table 1, dimensionless form of operating variables is shown to provide Eqs. 7 and 8 with V and Q. The variables r and v_{fr} stand for volume ratio of region 1 to 2 and fractional volume change which can be expressed as $v_{fr} = \theta\beta/4$.

The mean conversion for one period is

$$1 - \bar{S}_1 = \int_o^1 (1 - S_1)dt \quad \text{for modes I and III} \tag{9}$$

$$1 - \bar{S}_1 = \frac{1}{Q_{of} + Q_{ob}} \times \left[Q_{of}\int_o^\alpha (1 - S_1)dt + Q_{ob}\int_\alpha^1 (1 - S_1)dt\right] \quad \text{for mode II} \tag{10}$$

The nonlinear coupled Eqs. 7 and 8 preclude a simple solution so that two limiting forms of Eqs. 7 and 8 are considered to obtain analytical solutions. The problem is first solved for the high Damköhler number ($\lambda^2/\beta \gg 1$), and secondly for the high convective permeation velocity ($\beta \gg 1$) with first-order kinetics. Numerical solution is also presented for the original nonlinear equations.

Fast Reaction ($\lambda^2/\beta \gg 1$)

For a fast reaction, Eq. 7 becomes

$$\frac{d(V_1S_1)}{dt} = -\frac{\theta\hat{\beta}}{e^{\beta} - 1}e^{\hat{\beta}}S_1 + Q_i - Q_oS_1 \tag{11}$$

The appropriate initial conditions for Eq. 11 are

$$S_{1f}^i = S_{1b}|t=1 \tag{12}$$

$$S_{1b}^i = S_{1f}|t=\alpha \tag{13}$$

Solving Eq. 11 leads to the general solution with unknown initial substrate concentration:

$$S_1 = (S_1^i - g_1/g_2)g_3(t) + g_1/g_2 \tag{14}$$

where the functions g_1, g_2 and g_3 are given in Table 2. Using Eqs. 12 and 13, initial conditions for Eq. 14 can be obtained by solving the algebraic equations given below:

$$S_{1f}^i = (S_{1b}^i - g_{1b}/g_{2b})g_{3b}(1) + g_{1b}/g_{2b} \tag{15}$$

$$S_{1b}^i = (S_{1f}^i - g_{1f}/g_{2f})g_{3f}(\alpha) + g_{1f}/g_{2f} \tag{16}$$

High Ultrafiltration with First-order Kinetics ($\beta \gg 1$)

From now on, solutions of governing equations for mode III will be only presented for brevity and the reason will be discussed later. Solutions for the other modes can be obtained through the same mathematical manipulation. Neglecting diffusion in favor of convection makes Eqs. 7 and 8

$$\frac{dS_1}{dt} = -\theta\beta_fS_1 + F + \theta\beta_f - FS_1 \tag{17}$$

$$\frac{d(V_2S_2)}{dt} = \theta\beta_fS_1 - \theta\lambda^2S_2/K_m \tag{18}$$

during forward cycle, and

$$\frac{dS_1}{dt} = \theta\beta_bS_2 + F - \theta\beta_b - FS_1 \tag{19}$$

$$\frac{d(V_2S_2)}{dt} = -\theta\beta_bS_2 - \theta\lambda^2S_2/K_m \tag{20}$$

TABLE 2. EXPRESSION OF FUNCTIONS GIVEN IN EQ.

Mode	Time	g_1	g_2	g_3
I	Forward	F	$F + \theta\beta_f/(e^{\beta_f} - 1)$	$((1 + \theta\beta/4 - \theta\beta_f t)/(1 + \theta\beta/4))^{g_{2f}/\theta\beta_f}$
	Backward	F	$F - \theta\beta_b/(e^{-\beta_b} - 1)$	$((1 - \theta\beta/4)/(1 - \theta\beta/4 + \theta\beta_b(t - \alpha)))^{g_{2b}/\theta\beta_b}$
II	Forward	F	$F + \theta\beta_f/(e^{\beta_f} - 1)$	$e^{-g_{2f}t}$
	Backward	F	$F - \theta\beta_b/(e^{-\beta_b} - 1)$	$e^{-g_{2b}(t - b)}$
III	Forward	$F + \theta\beta_f$	$F + \theta\beta_f e^{\beta_f}/(e^{\beta_f} - 1)$	$e^{-g_{2f}t}$
	Backward	$F - \theta\beta_b$	$F - \theta\beta_b e^{-\beta_b}/(e^{-\beta_b} - 1)$	$e^{-g_{2b}(t - \alpha)}$

during backward cycle.

The initial conditions for S_1 and S_2 are the same as given in Eqs. 12 and 13.

Equation 17 yields

$$S_{1f} = (S'_{1f} - 1)\exp(-(F + \theta\beta_f)t) \tag{21}$$

which is substituted into Eq. 18 and the result reads to be

$$S_{2f} = (S'_{1f} - 1)(C_1(C_2 + \theta\beta_f t))^{-C_3} \times \exp(C_1C_2)(\gamma(C_3,C_1(C_2 + \theta\beta_f t)) - \gamma(C_3,C_1C_2)) + S'_{2f}(1 + \theta\beta_f t/C_2)^{-C_3} + (1 - (1 + \theta\beta_f t/C_2)^{-C_3})/C_3 \tag{22}$$

where $C_1 = F/\theta\beta_f + 1$, $C_2 = r - \theta\beta_f/4$, $C_3 = 1 + \lambda^2/K_m\beta_f$, and γ is the incomplete Gamma function (Abramowitz, 1965).

The solution of Eq. 20 is given by

$$S_{2b} = S'_{2b}(1 - \theta\beta_b(t - \alpha)/C'_2)^{C'_3 - 1} \tag{23}$$

where $C'_2 = r + \theta\beta_b/4$ and $C'_3 = 1 + \lambda^2/K_m\beta_b$

Substituting Eq. 23 into Eq. 19 leads to

$$S_{1b} = S'_{2b}C'_2(C'_1C'_2)^{-C'_3}\exp(-F(t - \alpha) + C'_1C'_2)(\gamma(C'_3,C'_1C'_2) - \gamma(C'_3,C'_1(C'_2 - \theta\beta_b(t - \alpha))) + S'_{1b}\exp(-F(t - \alpha)) + (1 - 1/C'_1)(1 - \exp(-F(t - \alpha))) \tag{24}$$

where $C'_1 = F/\theta\beta_b$.

Following the procedure in the previous fast reaction case, four algebraic equations appear with four unknowns

$$S'_{1f} = S_{1b|t=1}, \quad S'_{2f} = S_{2b|t=1}$$
$$S'_{1b} = S_{1f|t=\alpha}, \quad S'_{2b} = S_{2f|t=\alpha} \tag{25}$$

The solution is easily obtained by usual elimination method.

Nonlinear Kinetics

To solve the nonlinear coupled problem, a Runge-Kutta scheme is utilized with arbitrary initial substrate concentrations. After some transient period, steady cyclic motion of concentration is observed, the numerical integration is stopped at that point.

RESULTS AND DISCUSSION

Fast Reaction

In this regime, the substrate concentration of region 2 drops practically to zero. This diffusion-controlled region is very convenient where we can examine the role of ultrafiltration. Four dimensionless parameters F, α, β, and θ are needed to test fast reaction model. Therefore, to have some idea on the magnitude of these parameters, the data of Cross et al. (1971) for hollow fiber are presented below.

$u = O(10^{-5})$ m/s at 10^5Pa pressure difference

$u_d = O(10^{-6})$ m/s

Operating and geometric parameters are set as follows:

$T = O(10^2)$s

$\bar{Q}^* = O(10^{-5})$ m^3/s

$\bar{V}_1^* = O(10^{-5})$ m^3

$A = O(10^{-1})$ m^2

In Figure 3, the concentration histories in the three modes are plotted. The amplitude of mode III is the largest among the three modes since the concentration is largely affected by the fluctuating inlet flow rate. In other words, the substrate reservoir in mode III receives fresh substrate solution during the forward cycle at a higher flow rate than that in mode I or II and likewise less substrate solution during the backward cycle. Consequently this gives a larger fluctuation in the substrate concentration as compared with that in mode I or II. The concentration histories from modes I and II fluctuate in the nearly same manner. The slight difference observed between the concentration histories of modes I and II is due to the dissimilarity of mixing effects between the CSTR with a volume change and that with a constant volume. The calculations using Eqs. 9 and 10 have shown that the conversions in modes II and III are the same and the conversion of mode I is a little lower than that of modes II and III. Figure 4 shows a typical case for comparing mode I with modes II and III. Varying the period T automatically changes the parameters F and θ. At the same time, v_{fr}, which is $\theta\beta/4$, changes from 0.0125 to 0.75. At a higher v_{fr}, the conversion of mode I is a bit lower than that of modes II and III.

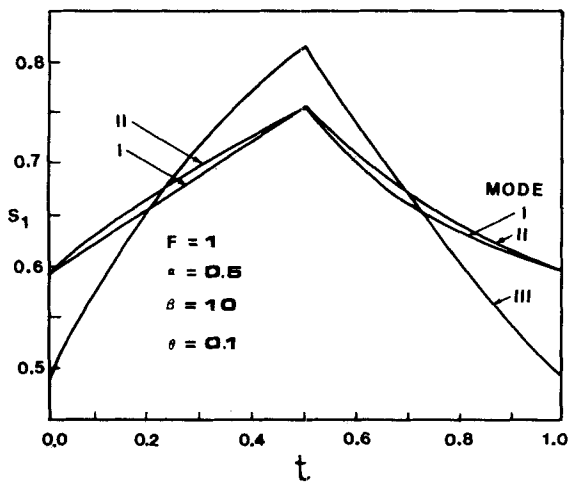

Figure 3. Concentration histories in modes I, II, and III at cyclic steady state.

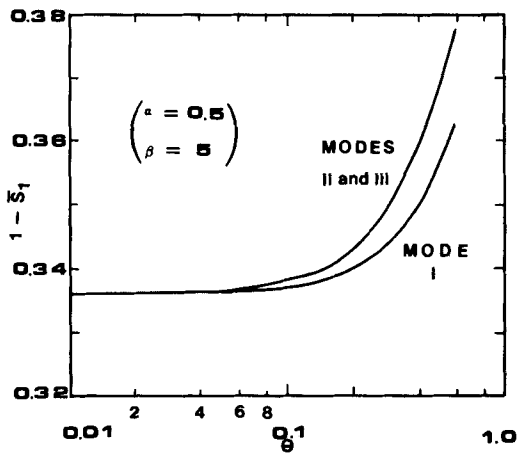

Figure 4. Comparison of modes I, II, and III with variation of period T.

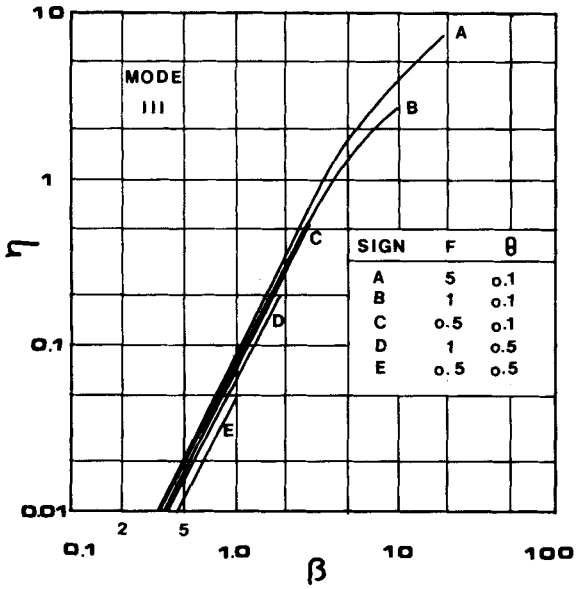

Figure 5. Relative increases of conversion over that without ultrafiltration for mode III in fast reaction (base conversions: $A = 0.0196$, $B = 0.091$, $C = 0.167$, $D = 0.333$, $E = 0.5$).

This can be ascribed to the fact that volume change of substrate reservoir reduces the efficiency of the reactor. As to the effect of frequency on the reactor performance, higher conversion is attained by increasing the period T. Because of the expected experimental convenience, mode III will be considered in the remaining part of this paper in favor of modes I and II.

When the substrate is transported only by diffusion, β equals zero and Eq. 3 becomes

$$J_s = u_d(S_1^* - S_2^*) \tag{26}$$

In this instance time has no meaning, and at steady state Eqs. 7 and 8 become

$$0 = -\theta(S_1 - S_2) + F(1 - S_1) \tag{27}$$

$$0 = \theta(S_1 - S_2) - \theta\lambda^2 S_2/(K_m + S_2) \tag{28}$$

Solving Eqs. 27 and 28 for S_1 and S_2, we obtain one more limiting solution.

$$S_1 = \tfrac{1}{2}((1 - K_m - \phi) + ((1 - K_m - \phi)^2 + 4K_m)^{1/2}) \tag{29}$$

$$1 - S_1 = (\theta/(\theta + F))(1 - S_2) \tag{30}$$

where $\phi = \lambda^2(1 + \theta/F)$.

Using Eqs. 29 and 30, minimum conversion is calculated, over which relative increase in conversion in terms of log (η) vs. log (β) is plotted in Figure 5. The curves terminate at the points where β is less than the mean flow rate F. The relative increase shows a rather similar trend for different mean flow rate and membrane permeability. For a high minimum conversion (case E) which is operated at a lower flow rate, relatively a small increase is obtained since the maximum filtrate which can be ultrafiltered is limited by the inlet flow rate. The curves are essentially straight lines below approximately $\beta = 2$, where the dominant transport mechanism changes from diffusion to convection.

High Ultrafiltration with First-Order Kinetics

In Figure 6 the mean value of S_1 during one period is plotted as a function of log (λ^2) with β as a parameter. The values of λ^2 and β given in the figure cover the practical operating conditions of reactor under diffusion controlled condition. For a large Damköhler number $\bar{S}_1$ reaches rapidly a diffusion controlled limit whose asymptotic values are given by Eq. 14. Under these conditions, ultrafiltration is very effective to enhance the conversion. At a higher β more substrate is available for reaction. As a result more

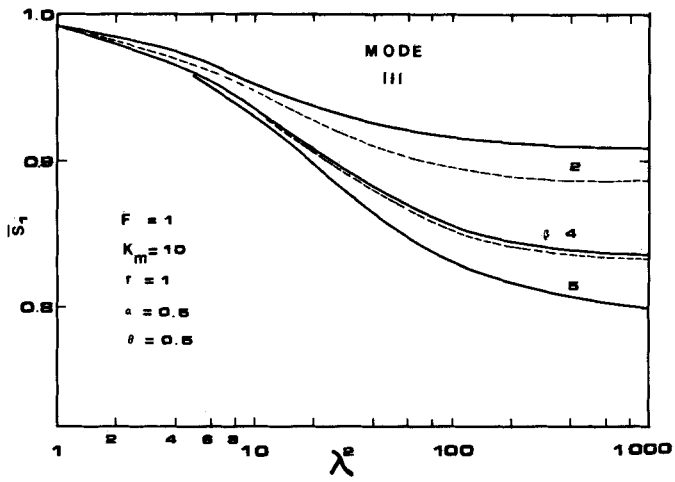

Figure 6. Effect of β on conversion of mode III in diffusion-controlled region (——— analytical solution from first-order high ultrafiltration model; - - - - - numerical solution from first-order general equation).

product appears in outflow, which leads to higher conversion. The validity of the analytical solution is confirmed by comparing with the numerical result of the general model with first-order kinetics in Figure 6. Unless β is large enough to neglect the diffusion contribution, for example, at $\beta = 2$ there is a discrepancy between the high ultrafiltration model and the general model.

Nonlinear Kinetics

The profiles of $\bar{S}_1$ vs. log (λ^2) for the nonlinear case qualitatively resemble those obtained from the high ultrafiltration model. The effect of ultrafiltration is once more seen in Figure 7 for K_m varying from 0.1 to 10. Waterland et al. (1974) pointed out that the transition region between the conditions of diffusion and kinetic controls is dependent on K_m. This nature is also observable in Figure 7. As K_m decreases, the transition region occurs over a narrow range of the Damköhler number.

The effect of dimensionless mean flow rate is shown in Figure 8. Since F has to be greater than $\theta\beta$, there is a limit to which β can vary. So it is convenient to operate the enzyme reactor at a high F. Moreover, we can obtain an appropriate conversion by varying β. For example, if F is held at 5 and β is increased to 5, we can attain a half of the conversion that is possible at $F = 0.5$. In this case the conversion decreases only by a factor of 0.5 despite of an order of magnitude increase in flow rate. Hence the productivity can increase fivefold.

The result of numerical study showed that nonlinear kinetics with $K_m \geq 10$ can be practically substituted by first-order kinetics without losing a great deal of accuracy.

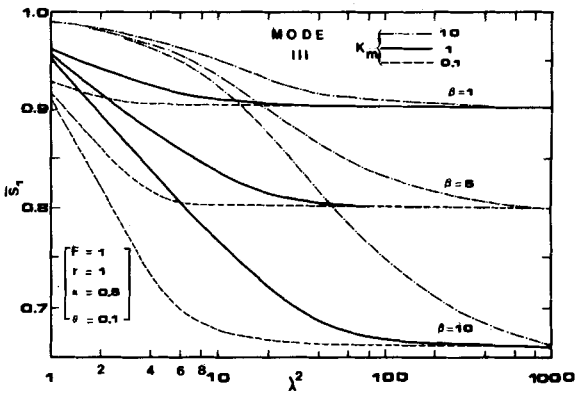

Figure 7. Effect of Michaelis constant on the shape of $\bar{S}_1$ vs. log (λ^2).

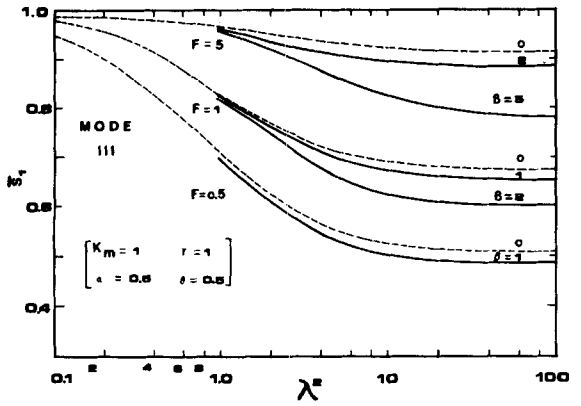

Figure 8. Performance of variable volume enzyme reactor as a function of flow rate.

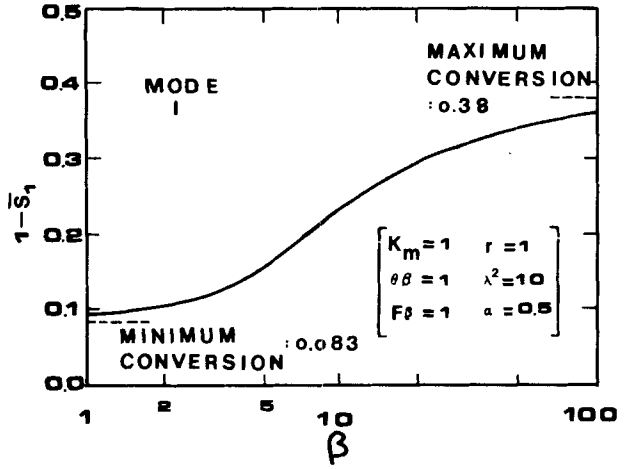

Figure 9. Comparison of CSTR with mode I in view of conversion.

CONCLUDING REMARKS

It seems appropriate to explain the continuous flow membrane enzyme reactor in comparison with CSTR. If the resistance through the membrane can be reduced by increasing β and decreasing T under the condition of $\theta\beta$, $F\beta$ being constant as in Figure 9, the conversion increases and reaches the asymptote which can be derived as follows. Assuming no transport limitation through the membrane, J_s will be infinite and at steady state S_1 will be equal to S_2. Combining Eqs. 7 and 8 for mode I and solving $\bar{S}_1$, we have

$$\bar{S}_1 = \tfrac{1}{2}((1 - K_m - \lambda^2\theta/rF) + ((-1 + K_m + \lambda^2\theta/rF)^2 + 4K_m)^{1/2}) \quad (31)$$

Equation 31 shows the conversion of CSTR when enzyme is not washed out. Thus this conversion will be the maximum steady-state conversion for the given reaction conditions. On the other hand, the minimum conversion is given by Eqs. 29 and 30.

Increasing β in modes II and III is not as feasible as in mode I owing to the condition of $F > \theta\beta$ in the flow swing operation. To circumvent this limitation, two-step semibatch or three-step batch operation (forward ultrafiltration, reaction, and backward ultrafiltration) can be considered. The results of these schemes will be reported in the subsequent paper.

Michaels (1980) indicates that hollow-fiber devices are most promising reactors for immobilized enzymes and mammallian cell culture. In order that the hollow-fiber may be used as an enzyme reactor, enzymes are placed in the shell side of fibers and substrate solution flows through the lumen. The substrate is supplied to enzyme by diffusion and convection. Since the diffusion is much slower process than convection, it is more convenient to carry substrate by forcing substrate solution to flow convectively through membrane. Here a method must be devised to reduce the increased volume of the shell side, and suction into the lumen may be a good solution. In this way, a new flow swing method is developed to replace the pressure swing and theoretically proved more efficient.

Still a remaining problem is to improve the stability of soluble enzyme and to prevent the leaking of enzyme through the fiber walls due to the uneven distribution of membrane pore size. However, these problems can be solved by further investigation of making soluble enzyme stable for a long period (Schmid, 1979) and by increasing the physical size of soluble enzyme by attaching dextran or water soluble polymers to enzyme. In summary, a hollow-fiber enzyme reactor with ultrafiltration swing has two distinct advantages over other reactors: The enzyme activity may be increased infinitely without suffering from diffusion limitation through membrane; secondly the immobilization procedure is simpler than any other methods.

NOTATION

A = membrane area, m^2
D = substrate diffusivity, m^2/s
F = dimensionless mean flow rate
F_m^* = DA/l m^3/s
J_s = solute flux, $mol/m^3/m^2/s$
J_v = solvent flux, m/s
k = a constant in Eq. 1, m/Pa/s
K_m = Michaelis constant, mol/m^3
l = effective diffusion length, m
O = sign for order of magnitude
p = pressure, Pa
Q = flow rate
r = ratio of volume of enzyme solution to that of substrate solution
S = substrate concentration
t = time
T = period, s
u = convective velocity, m/s
u_d = diffusive velocity, m/s
v_{fr} = fraction of volume change to mean volume of substrate solution
V = volume
V_m = maximum enzyme reaction rate, $mol/m^3/s$
z = coordinate perpendicular to membrane surface

Greek Letters

α = dimensionless forward cycle time
β = u/u_d
Δ = difference operator
η = (conversion of $\beta \neq 0$ − conversion of $\beta = 0$)/conversion of $\beta = 0$
θ = $F_m^* T/\bar{V}_1^*$
λ^2 = Damköhler number defined by $V_m \bar{V}_2^*/K_m F_m^*$

Superscripts

i = initial value
$\bar{}$ = mean value
$*$ = dimensional quantity
$\hat{}$ = vector quantity

Subscripts

b = backward cycle
f = forward cycle
i = inlet
o = outlet
1,2 = substrate and enzyme side, respectively

Mathematical Operator

$$\gamma(a,x) = \int_o^x \exp(-x)x^{a-1}dx$$

LITERATURE CITED

Abramowitz, M., and I. A. Stegum, eds., *Handbook of Mathematical Functions*, p. 255, Dover Publications, Inc., New York (1965).

Alfani, F., G. Iorio, G. Greco, Jr., M. Cantarella, M. H. Remy, and V. Scardi, "Kinetic Behavior of Immobilized Enzyme Membrane Reactors," *Chem. Eng. Sci.*, **34**, 1213 (1979).

Bean, C. P., "The Physics of Porous Membranes-Neutral Pores," *Membranes*, **1**, p. 1, G. Eisenman, ed., Marcel Dekker, Inc., New York (1972).

Butterworth, T. A., D. I. C. Wang, and A. J. Sinskey, "Application of Ultrafiltration for Enzyme Retention during Continuous Enzymatic Reaction," *Biotech. Bioeng.*, **12**, 615 (1970).

Chang, H. N., and I. H. Kim, "A Theoretical Analysis on the Performance of Membrane/Enzyme Reactor with Pressure Swing," *Proceedings of 2nd World Congress of Chemical Engineering*, Montreal, Canada, p. 256 (Oct. 4–9, 1981).

Cross, R. A., W. H. Tyson, Jr., and D. S. Cleveland, "Asymmetric Hollow Fiber Membranes for Dialysis," *Trans. Amer. Soc. Art. Int. Organs*, **17**, p. 279 (1971).

Furusaki, S., T. Kojima, and T. Miyauchi, "Reaction by the Enzyme Entrapped by UF Membrane with Acceleration of Mass Transfer by Pressure Swing," *J. Chem. Eng. Japan*, **10**, p. 233 (1977).

Ku, K., M. J. Kuo, J. Delente, B. S. Wildi, and J. Feder, "Development of a Hollow-Fiber System for Large-Scale Culture of Mammalian Cells," *Biotech. Bioeng.*, **23**, p. 79 (1981).

Michaels, A. S., "Membrane Technology and Biotechnology," *Desalination*, **35**, p. 329 (1980).

Rony, P. R., "Multiphase Catalysis II. Hollow Fiber Catalysis," *Biotech. Bioeng.*, **13**, p. 431 (1971).

Schmid, R. D., "Stabilized Soluble Enzymes," in *Adv. in Biochem. Eng.*, **12**, p. 41, T. K. Ghose, A. Fiechter, and N. Blakebrough, eds., Springer Verlag, Heidelberg (1979).

Waterland, L. R., A. S. Michaels, and C. R. Robertson, "A Theoretical Model for Enzymatic Catalysis Using Asymmetric Hollow Fiber Membranes," *AIChE J.*, **20**, p. 50 (1974).

Manuscript received November 5, 1981; revision received May 25, and accepted June 18, 1982.

Occurrence of Methane Hydrate in Saturated and Unsaturated Solutions of Sodium Chloride and Water in Dependence of Temperature and Pressure

Experimental results of the formation of methane hydrate in dependence of temperature and pressure in unsaturated solutions of NaCl in water will be presented in a temperature range from 261.85 to 285.98 K and pressure up to 11.0 MPa. Furthermore the four-phase equilibrium $NaCl{\cdot}2H_2O_S$–$CH_4{\cdot}nH_2O_S$–L–G has been calculated from the experimental results. Also the heats of transformation of several other equilibria in the ternary system CH_4–H_2O–NaCl are obtained.

J. L. de ROO, C. J. PETERS, R. N. LICHTENTHALER, and G. A. M. DIEPEN

Department of Chemistry
Delft University of Technology
Delft, The Netherlands

SCOPE

At present there are several regions of industrial interest where gas hydrates play a role. Another possibility to apply gas hydrates, which can become of industrial interest, is the storage of natural gas as hydrates in salt holes in the crust of the earth. This application of gas hydrates requires knowledge of the conditions of hydrate formation. If we should store natural gas in salt holes as hydrates, the three components will be present: methane, water and sodium chloride. For this reason the phase behavior of the ternary system CH_4–H_2O–NaCl, especially in the region where the methane hydrate occurs, is investigated.

To achieve this, we measured temperature and pressure values at which methane hydrate just disappeared in the presence of an unsaturated solution of NaCl in water as the liquid phase and nearly pure methane as the vapor phase. From these measurements the p,T-projection of the invariant and the univariant equilibria in the ternary system CH_4–H_2O–NaCl will be derived. The measurements were carried out in a Cailletet equipment in a temperature region from 261.85 to 285.98 K and pressures up to 11.0 MPa.

CONCLUSIONS AND SIGNIFICANCE

The measurements allowed us to calculate the invariant as well as the univariant equilibria of the ternary system CH_4–H_2O–NaCl. To obtain a higher accuracy, direct measurement of the univariant equilibria has to be preferred over the experimental and calculation procedures here. The accuracy will then largely depend on the possible accuracy of the experimental equipment. Nevertheless, we were able to derive the p,T-projection of the ternary system CH_4–H_2O–NaCl with reasonable accuracy. Furthermore, the composition of the methane hydrate was calculated.

Correspondence concerning this paper should be addressed to C. J. Peters